Rosuvastatin Attenuates Pulmonary Damage in Rats with Cecal Ligation and Puncture-Induced Sepsis

Safiye İnşira Yıldız , Faruk Saydam * , Atilla Topçu , Levent Tümkaya , Eda Yılmaz Kutlu , Hüseyin Avni Uydu

Posted Date: 5 May 2026

doi: 10.20944/preprints202605.0139.v1

Keywords: sepsis; inflammation; rosuvastatin; lung; rat

 doi:10.20944/preprints202605.0139.v1

Article

Rosuvastatin Attenuates Pulmonary Damage in Rats with Cecal Ligation and Puncture-Induced Sepsis

Safiye İnşira Yıldız [1], Faruk Saydam [2,*], Atilla Topçu [3], Levent Tümkaya [4], Eda Yılmaz Kutlu [5] and Hüseyin Avni Uydu [6]

[1] Health Institutes of Türkiye (TÜSEB), Ankara, Türkiye
[2] Department of Medical Biology, Faculty of Medicine, Recep Tayyip Erdogan University, Rize, Türkiye
[3] Department of Pharmacology, Faculty of Medicine, Recep Tayyip Erdogan University, Rize, Türkiye
[4] Department of Histology and Embryology, Faculty of Medicine, Ondokuz Mayıs University, Samsun, Türkiye
[5] Department of Medical Biochemistry, Faculty of Medicine, Recep Tayyip Erdogan University, Rize, Türkiye
[6] Department of Medical Biochemistry, Faculty of Medicine, Samsun University, Samsun, Türkiye
* Correspondence: faruk.saydam@e-mail.com; Tel.: (+90) 505 2419232

Abstract

Background/Objectives: Sepsis is a life-threatening condition characterized by a dysregulated host immune response, frequently leading to multiple organ dysfunction, with the lungs being among the most severely affected organs. Oxidative stress, inflammation, apoptosis, and DNA damage play key roles in the pathogenesis of sepsis-induced acute lung injury (ALI). Beyond its lipid-lowering effects, rosuvastatin possesses anti-inflammatory and antioxidant properties that may confer protective effects in sepsis. This study aimed to evaluate the dose-dependent effect of rosuvastatin against pulmonary damage in an experimental model of sepsis induced by cecal ligation and puncture (CLP). **Methods:** Sprague–Dawley rats were randomly divided into six groups: Sham, Sham + rosuvastatin (10 mg/kg), Sham + rosuvastatin (20 mg/kg), CLP, CLP + rosuvastatin (10 mg/kg), and CLP + rosuvastatin (20 mg/kg). Rosuvastatin was administered via oral gavage before 4 hours the CLP procedure in the experimental groups. All rats were euthanized 16 hours after induction of CLP. Lung tissues were analyzed for biochemical markers, including malondialdehyde (MDA) and reduced glutathione (GSH), as well as histopathological changes and immunohistochemical expression of NF-κB/p65, caspase-3, and 8-OHdG. **Results:** CLP-induced sepsis significantly increased MDA levels while decreasing GSH levels, indicating enhanced oxidative stress. Rosuvastatin treatment significantly reversed these changes. Histopathological analysis revealed marked lung injury in the CLP group, including alveolar inflammation, interstitial inflammation, vascular congestion, and increased alveolar septal thickness, all of which were significantly reduced following rosuvastatin administration. Immunohistochemical findings demonstrated increased expression of NF-κB/p65, caspase-3, and 8-OHdG in the CLP group, whereas rosuvastatin significantly attenuated these expressions. No significant differences were observed between the two rosuvastatin doses. **Conclusion:** Rosuvastatin exerts significant protective effects against sepsis-induced lung injury by reducing oxidative stress, inflammation, apoptosis, and DNA damage. These findings suggest that rosuvastatin may have therapeutic potential in the management of sepsis-associated pulmonary injury, although further studies are required to confirm its clinical applicability.

Keywords: sepsis; inflammation; rosuvastatin; lung; rat

1. Introduction

Sepsis is a life-threatening syndrome caused by a dysregulated host response to infection, frequently resulting in multiple organ dysfunction and high global mortality rates [1]. Recent data

 doi:10.20944/preprints202605.0139.v1

indicate that sepsis accounts for approximately 48.9 million cases and 11 million deaths worldwide annually [2]. Chronic inflammatory processes and organ failures constitute primary contributors to the elevated mortality rates associated with sepsis. The lungs are among the most frequently and severely affected organs in sepsis. A considerable proportion of patients develop acute lung injury (ALI), which, if not adequately controlled, may progress to acute respiratory distress syndrome (ARDS) [3]. It has been reported that monocytes and macrophages contribute to the pathogenesis of sepsis by mounting an immune response against pathogens through the expression of several pro-inflammatory cytokines, including tumor necrosis factor-alpha (TNF-α), interleukin-6 (IL-6), interleukin-1 beta (IL-1β), and interleukin-10 (IL-10) [4]. Reactive oxygen species (ROS), including superoxide anions, hydrogen peroxide, peroxynitrite, hypochlorous acid, and hydroxyl radicals, promote the expression of these cytokines primarily through activation of the nuclear factor kappa B (NF-κB) signaling pathway. Moreover, activated pro-inflammatory cytokines upregulate the expression of ROS-generating enzymes, thereby promoting excessive ROS production [5]. Antioxidant defense systems counteract excessive ROS by enzymatically detoxifying reactive intermediates, principally through the coordinated actions of superoxide dismutase (SOD), glutathione reductase (GR), glutathione peroxidase (GSH-Px), and catalase (CAT). Dysregulated cytokine overproduction, in turn, disrupts cellular energy metabolism and compromises endothelial integrity, leading to increased vascular permeability and impaired tissue perfusion [6].

Apoptosis in lung tissue during sepsis develops because of structural and functional damage induced by an excessive inflammatory response affecting the alveolar epithelium and pulmonary microvascular endothelium. During sepsis, circulating mediators such as tumor TNF-α, IL-1β, IL-6, Fas ligand, and others activate both the extrinsic death receptor–mediated apoptotic pathway and the intrinsic mitochondrial stress–associated pathway; the convergence point of these pathways is the activation of caspase-3 [7,8]. Apoptosis of type I and type II pneumocytes disrupts alveolar fluid clearance and impairs gas exchange, whereas endothelial cell apoptosis promotes increased vascular permeability, interstitial and alveolar edema, and inflammatory cell infiltration [9].

During sepsis, activated neutrophils, macrophages, and injured pulmonary cells generate excessive amounts of ROS and reactive nitrogen species (RNS); these molecules induce oxidative damage to nuclear and mitochondrial DNA, including base oxidation, single- and double-strand breaks, and other oxidative modifications [10,11]. In this context, 8-hydroxy-2′-deoxyguanosine (8-OHdG) is one of the most used biomarkers and is widely recognized as a reliable indicator of oxidative DNA damage [12]. Pulmonary DNA damage, reflected by increased 8-OHdG levels and mitochondrial genomic injury, is closely associated with the induction of apoptosis; this process ultimately disrupts alveolar epithelial and endothelial integrity, promotes edema formation and impaired gas exchange, and may progress to ALI and ARDS [13].

Despite advances in supportive care, effective therapies specifically targeting sepsis-induced pulmonary injury remain limited, underscoring the need for novel interventions [14]. Experimental animal models are essential for studying sepsis pathophysiology and evaluating therapeutic agents. The cecal ligation and puncture (CLP) model is considered the standard in rodents, as it closely replicates the polymicrobial infection and systemic inflammation seen in humans. The CLP model reliably induces bacteremia, cytokine storm, and organ dysfunction, making it highly suitable for preclinical studies of sepsis and organ-protective strategies [15].

Statins are distinguished not only by their lipid-lowering properties but also by their pleiotropic effects, including anti-inflammatory, antioxidant, immunomodulatory, and endothelial-protective activities. These biological actions suggest their potential as therapeutic agents in inflammatory pathologies such as sepsis [16,17]. Preclinical and clinical studies indicate that statins may improve outcomes in sepsis by modulating inflammatory pathways, reducing oxidative stress, and preserving organ function [18,19]. Rosuvastatin is a widely prescribed 3-hydroxy-3-methylglutaryl-CoA (HMG-CoA) reductase inhibitor, primarily used for the treatment of dyslipidemia and to reduce cardiovascular risk. Compared to other molecules in the same class, rosuvastatin has been reported to exhibit high efficacy in improving lipid profiles. Through its anti-inflammatory, antioxidant, and antithrombotic effects, it serves as an important agent for both primary and secondary prevention of

 doi:10.20944/preprints202605.0139.v1

cardiovascular disease [20]. These properties of rosuvastatin have been demonstrated to attenuate oxidative stress and systemic inflammation in various experimental animal models [21,22]. In lung tissue exposed to LPS-induced inflammation, rosuvastatin significantly decreased proinflammatory enzymes such as iNOS and COX-2 and reduced histopathological damage. Furthermore, the study demonstrated a marked decrease in the concentrations of key cytokines, including TNF-α, IL-6, and IL-1β, in both plasma and tissue samples [23]. However, the specific effects of rosuvastatin on sepsis-induced pulmonary injury, particularly in the CLP model, have not been fully characterized. This study aims to evaluate the protective effects of rosuvastatin on lung tissue in rats with sepsis induced by CLP, by analyzing key cellular parameters involved in oxidative stress, apoptosis, and inflammatory pathways.

2. Materials and Methods

2.1. Experimental Animals

Ethical approval for this study was obtained from the Local Ethics Committee for Animal Experiments of Recep Tayyip Erdoğan University (Approval Date: July 16, 2020; Decision No: 2020/32). The Scientific Research Projects Coordination Unit of Recep Tayyip Erdoğan University provided financial support for this research. Male Sprague-Dawley rats, 4–6 weeks of age and weighing 270–300 g, were used in this study. The animals were bred and housed at the Laboratory Animal Production and Research Center of Recep Tayyip Erdoğan University. All animals were maintained under standardized hygienic conditions in the experimental animal facility, with a controlled 12-hour light/12-hour dark cycle, a relative humidity of 55–60%, and an ambient temperature of 22 ± 2 °C. They had free access to tap water and standard pellet chow throughout the study.

2.2. Treatment Groups

A total of 60 rats were randomly assigned to six groups, with 10 animals per group, as follows: Sham, Sham + Rosuvastatin (10 mg/kg), Sham + Rosuvastatin (20 mg/kg), CLP, CLP + Rosuvastatin (10 mg/kg), and CLP + Rosuvastatin (20 mg/kg). In the Sham groups, a laparotomy was conducted by carefully exteriorizing the cecum, performing minimal manipulation, and subsequently returning it to the abdominal cavity before surgical closure. The Sham + Rosuvastatin groups received oral gavage of rosuvastatin (Crestor, AstraZeneca İlaç. San. ve Tic. Ltd. Şti., Istanbul, Türkiye) at 10 or 20 mg/kg 4 hours before the surgical procedure. In contrast, the Sham control group received an equivalent volume of 0.9% NaCl. In the CLP groups, sepsis was induced as described previously [24]. Rats in the CLP + Rosuvastatin groups were administered rosuvastatin at 10 or 20 mg/kg via oral gavage 4 hours before surgery, while the CLP control group received 0.9% NaCl. All animals were monitored postoperatively under standard laboratory conditions until the experimental endpoint, which was set at 16 hours following surgery administration. Sixteen hours after the surgical procedure, all animals were sacrificed under deep anesthesia induced by high-dose ketamine hydrochloride (Pfizer İlaçları Ltd. Şti., Istanbul, Türkiye) and xylazine hydrochloride (Rompun, Bayer, USA). The lung tissues were subsequently bisected longitudinally. One portion was preserved at −80 °C for biochemical analyses, while the other was fixed in 10% neutral-buffered formalin (Sigma-Aldrich, Saint Louis, MO, USA) for histological evaluation.

2.3. Cecal Ligation and Puncture (CLP) Model

All surgical procedures were conducted under sterile conditions. Rats were anesthetized via intraperitoneal injection of ketamine hydrochloride (50 mg/kg) and xylazine hydrochloride (10 mg/kg). Once adequate anesthesia was confirmed, a 2.5 cm midline abdominal incision was made. The cecum was carefully exteriorized, and a ligation was performed just distal to the ileocecal valve using 4/0 silk sutures. Two punctures were then created in the distal cecum with a 22-gauge needle to allow the release of cecal contents into the peritoneal cavity. Following this, the cecum was returned to the abdominal cavity, and the incision was closed in two layers using sterile, absorbable

 doi:10.20944/preprints202605.0139.v1

4/0 sutures. The surgical site was irrigated with 1% lidocaine (Onfarma, Samsun, Türkiye) to provide local analgesia.

2.4. Biochemical Analysis

2.4.1. Tissue Homogenization

A homogenization solution consisting of 20 mM sodium phosphate and 140 mM potassium chloride (KCl) at pH 7.4 was initially prepared. Subsequently, 1 mL of homogenization solution was added to 0.1 g of the tissue sample, and the mixture was then homogenized. The homogenates were subjected to centrifugation at 800 g for 10 minutes at 4 °C. The supernatants obtained were used to assess thiobarbituric acid-reactive substances (TBARS) and -SH levels.

2.4.2. TBARS Analysis

TBARS, a significant marker of tissue damage, serves as a critical indicator of oxidant stress that activates reactive oxygen species (ROS) through the oxidative stress pathway. This procedure was conducted according to the method outlined by Ohkawa et al [25]. In summary, to 200 µL of tissue supernatant, 50 µL of 8.1% sodium dodecyl sulfate, 375 µL of 20% acetic acid (v/v) (pH 3.5), and 375 µL of 0.8% thiobarbituric acid (TBA) were added. The mixture was vortexed and incubated for 1 h in a boiling water bath, followed by cooling in ice water for 5 min and centrifugation at 750 g for 10 min. The resulting pink color was analyzed using a spectrophotometer at 532 nm. The results were reported as nmol/mg tissue.

2.4.3. Total Thiol Group Analysis

-SH groups were determined using the Ellman reagent [26]. Briefly, 100 µL of 3 M Na_2HPO_4 and 25 µL of DTNB (5,5-dithiobis-(2-nitrobenzoic acid)) were added to 25 µL of supernatant. The DTNB solution contained 4 mg of DTNB dissolved in 10 mL of 1% sodium citrate solution. The yellow color emerging after gentle shaking was then subjected to spectrophotometric analysis at 412 nm. The results were calculated using standard graphs for 1000 µM to 62.5 µM reduced glutathione and were expressed as nanomoles per milligram of tissue.

2.5. Histopathological Analysis

Lung samples were fixed in 10% neutral-buffered formalin (Sigma-Aldrich, Saint Louis, MO, USA) for 24 hours. Following fixation, the tissues were dehydrated through a graded ethanol (Merck GmbH, Darmstadt, Germany) series according to standard histological protocols. Subsequently, the specimens were cleared in two changes of xylene (Merck GmbH, Darmstadt, Germany) and embedded in paraffin blocks (Isolab GmbH, Germany) using a tissue embedding system (Leica, EG1150, Germany). The sections were subsequently stained with Hematoxylin-Eosin (H&E, Harris hematoxylin Eosin G Merck GmbH, Darmstadt, Germany) using an automated tissue stainer (Leica ST5020, Germany). Following staining, the samples were examined under a light microscope (Olympus BX51, Olympus Corp., Japan), and images were captured with a digital camera mounted on the microscope.

Histopathological evaluation of H&E-stained sections was performed by two independent histologists, blinded to the experimental groups, who examined and scored thirty-five distinct microscopic fields for each animal. Lung tissue samples were evaluated for alveolar inflammation, interstitial inflammation, vascular congestion, and alveolar septal thickening. Alveolar septal wall thickness in the tissue sections was measured using the arbitrary probe tool of the Olympus DP 2.0 software (Figure 1, Olympus Corp., Japan). The lung damage score (LDS) was calculated according to the system described by Matute-Bello et al [27]. In this scoring method, the extent of tissue damage was assigned to a score of 0, 1, 2, or 3 based on the percentage of affected tissue. Alveolar septal thickening was scored by calculating the ratio of the treatment group to the sham group (Table 1).

 doi:10.20944/preprints202605.0139.v1

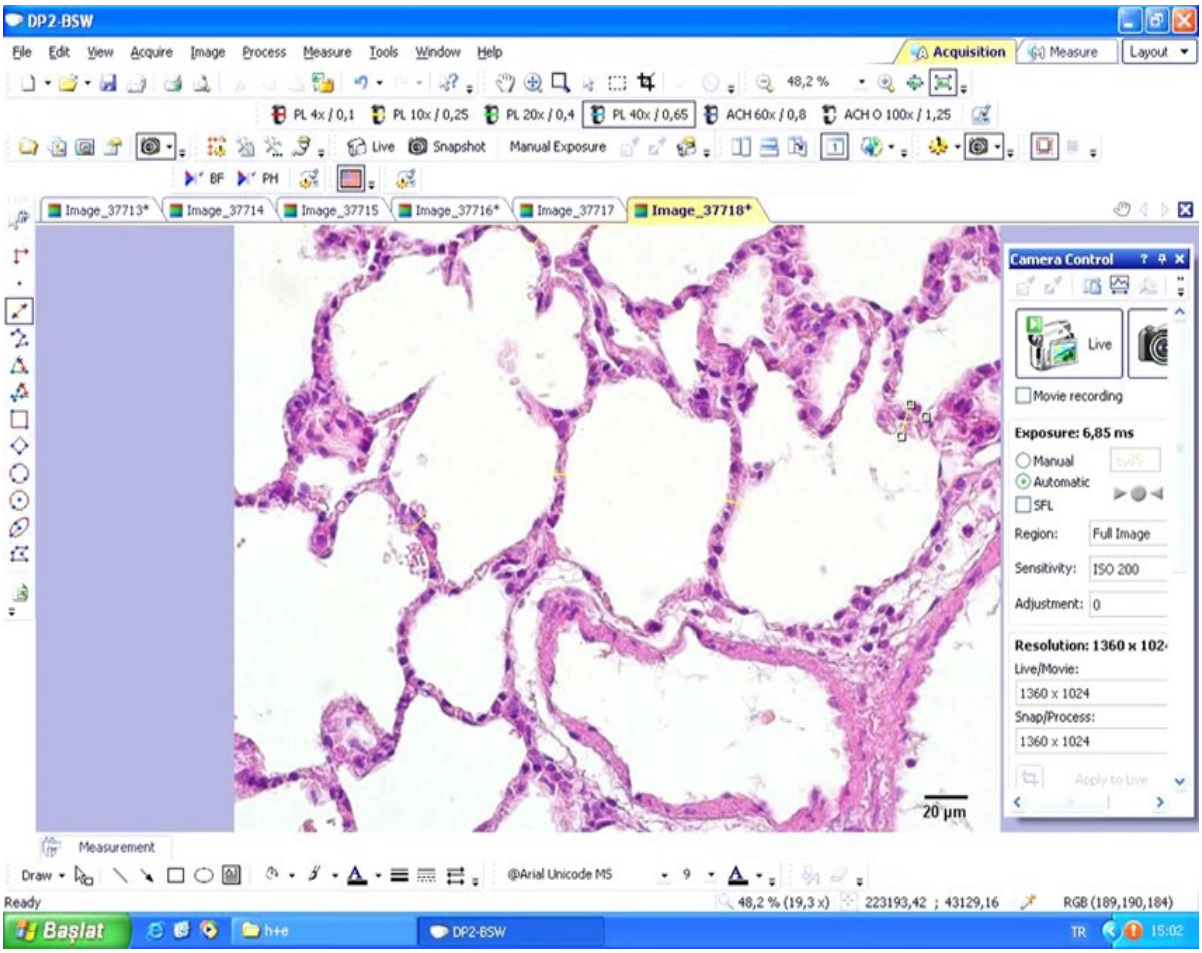

Figure 1. The Olympus DP 2.0 (Olympus Corp., Japan) software program, by which alveolar septal wall thickness was measured in tissue section images using an arbitrary probe.

Table 1. Lung Damage Score (LDS) as defined by Matute-Bello et al.

Findings	Score			
	0	1	2	3
Alveolar Inflammation	≤%5	%6-%25	%26-%50	≥%50
Interstitial Inflammation	≤%5	%6-%25	%26-%50	≥%50
Vascular Congestion	≤%5	%6-%25	%26-%50	≥%50
Alveolar Septal Thickening (Treatment Group/Sham Group Ratio)	≤X1	<X2	≥X2	≥X4

2.6. Immunohistochemical (IHC) Analysis

Primary antibodies were used to evaluate the inflammatory response (anti-NF-κB/p65, rabbit polyclonal, Abcam, ab16502, UK), to identify apoptotic pneumocytes (anti-caspase-3, rabbit polyclonal, Abcam, ab44976, UK), and to detect oxidative DNA damage (anti-8-OHdG [8-hydroxy-2-deoxyguanosine], rabbit polyclonal, Abcam, ab16502, UK). Detection was performed with an appropriate horseradish peroxidase-conjugated secondary antibody (Goat Anti-Rabbit IgG H&L (HRP), Abcam, ab205718, UK). Lung tissue paraffin sections, 2–3 µm thick, were mounted on positively charged slides (Patolab, PRC). After dehydration, the sections were treated with hydrogen

 doi:10.20944/preprints202605.0139.v1

peroxide to block endogenous peroxidase activity, following the protocols provided by the primary antibody kit manufacturers. Following deparaffinization and antigen retrieval performed using the Leica IHC/ISH system (Leica Biosystems, Germany), the tissue sections were incubated with the respective primary and secondary antibodies for 60 minutes each, in accordance with the manufacturer's standardized protocol. Immunoreactivity was visualized using diaminobenzidine tetrahydrochloride (Leica LTraview DAB, Leica Biosystems, Wetzlar, Germany), and the sections were counterstained with Harris hematoxylin (Merck, Darmstadt, Germany).

Immunopositive cells in the IHC-stained sections were evaluated using a semi-quantitative scoring system (Table 2). Two histologists, blinded to the experimental groups, independently assessed thirty-five randomly selected regions per section at 40× magnification.

Table 2. Immunohistochemical staining positivity scores.

Findings	Score	Percentage%
None	0	<%5
Mild	1	5-25%
Moderate	2	26-50%
Severe	3	%50>

2.7. Statistical Analysis

Statistical analyses were conducted using IBM SPSS Statistics version 23 (SPSS Inc., Chicago, IL, USA). Data distribution was assessed with the Kolmogorov–Smirnov test. The non-parametric data obtained from the semi-quantitative analysis were expressed as median with interquartile range. Between-group differences for continuous variables with a normal distribution were assessed using one-way analysis of variance (ANOVA) with Tukey's HSD post hoc test. Non-parametric variables were evaluated using the Kruskal–Wallis test followed by Tamhane's T2 post hoc test.

3. Results

3.1. Malondialdehyde (MDA) Levels

When MDA levels were analyzed, they were found to be significantly higher in the CLP group compared to the Sham group ($p < 0.05$). MDA levels were significantly lower in the CLP + 10 mg/kg rosuvastatin and CLP + 20 mg/kg rosuvastatin groups compared to the CLP group ($p<0.05$). No statistically significant difference was observed between the two rosuvastatin doses (10 mg/kg and 20 mg/kg). Detailed MDA data are presented in Table 3.

Table 3. Mean MDA levels of the experimental groups and the results of the statistical analysis.

Group	MDA (nmol/mg)
Sham	54.68 ± 1.6
CLP	92.56 ± 14.7[a]
CLP + 10 mg/kg Rosuvastatin	51.08 ± 6.5[b]
CLP + 20 mg/kg Rosuvastatin	57.40 ± 10.6[b]
Sham + 10 mg/kg Rosuvastatin	46.53 ± 3.2

 doi:10.20944/preprints202605.0139.v1

Sham + 20 mg/kg Rosuvastatin	51.50 ± 4.7

Data are expressed as mean ± standard deviation. Statistical analysis was performed using one-way ANOVA followed by Tukey's HSD test ([a] $p < 0.05$ vs. Sham group; [b] $p < 0.05$ vs. CLP group).

3.2. Reduced Glutathione (GSH) Levels

The analysis of GSH levels revealed a significant decrease in the CLP group compared to the Sham group ($p < 0.05$). Rosuvastatin treatment significantly increased GSH levels in the CLP groups ($p < 0.05$). No significant difference was observed between the two doses of rosuvastatin (10 mg/kg and 20 mg/kg). The GSH data are presented in Table 4.

Table 4. Mean GSH levels of the experimental groups and the results of the statistical analysis.

Group	GSH (nmol/mg)
Sham	19.05±2.8
CLP	12.75±1.7[a]
CLP + 10 mg/kg Rosuvastatin	19.53±3.4[b]
CLP + 20 mg/kg Rosuvastatin	19.04±3.8[b]
Sham + 10 mg/kg Rosuvastatin	18.72±3.6
Sham + 20 mg/kg Rosuvastatin	17.35±3.5

Data are expressed as mean ± standard deviation. Statistical analysis was performed using one-way ANOVA followed by Tukey's HSD test ([a] $p < 0.05$ vs. Sham group; [b] $p < 0.05$ vs. CLP group).

3.3. Histopathological Findings

Representative microscopic images of lung tissue samples evaluated for alveolar inflammation, interstitial inflammation, vascular congestion, and alveolar septal thickness are presented in Figure 2. The findings were evaluated according to the LDS system proposed by Matute-Bello et al [27]. The scores of the assessed lung tissue parameters were significantly higher in the CLP group compared to the other groups. Administration of rosuvastatin to septic rats resulted in a significant reduction in all scores. However, no significant dose-dependent difference was observed between the groups receiving 10 mg and 20 mg of rosuvastatin (Table 5).

 doi:10.20944/preprints202605.0139.v1

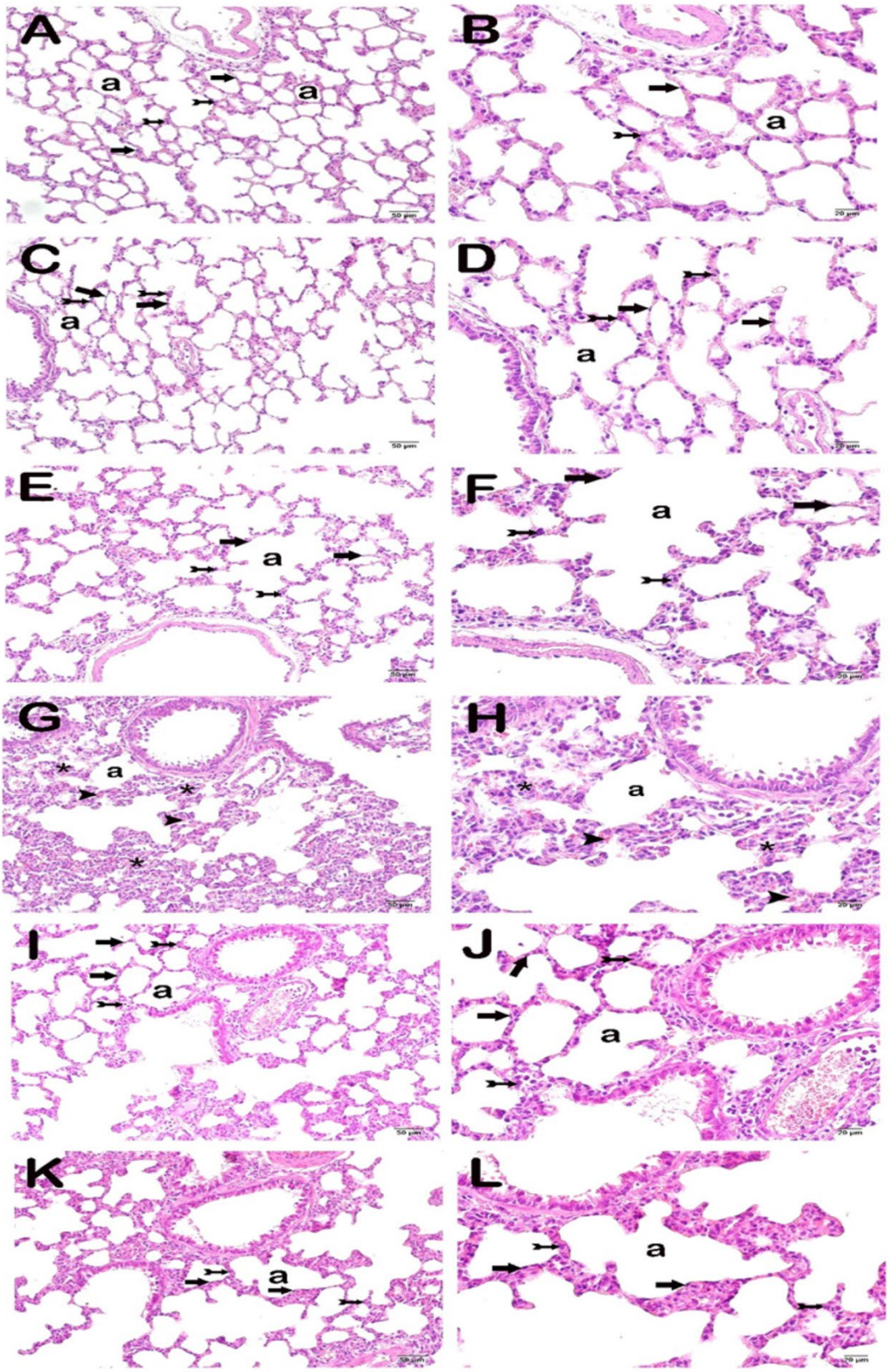

Figure 2. Representative light microscopic image of lung tissue sections stained with Harris hematoxylin and eosin G. Alveolus (**a**), type I pneumocyte (**arrow**), and type II pneumocyte (**arrowhead**). A (×20)-B (×40): In sections from the healthy control group, alveolar septal walls composed of normal type I pneumocytes (arrow) and type II pneumocytes were

 doi:10.20944/preprints202605.0139.v1

observed (LDS: 0 [0–0.5]). C (×20)-D (×40): In sections from the CR10 mg treatment group, alveolar septal wall structures with typical morphology were observed (LDS: 0 [0–1]). E (×20)-F (×40): In sections from the CR20 mg treatment group, alveolar (a) structures composed of morphologically normal type I pneumocytes (arrow) and type II pneumocytes (arrowhead) were observed (LDS: 1 [0–1]). G (×20)-H (×40): In sections from the CLP group, thickening of the alveolar septal walls (asterisk) was observed. In addition, widespread vascular congestion (arrowhead) was detected in the interstitial areas (LDS: 5 [4–7]). I (×20)-J (×40): In sections from the CLP+CR10 mg treatment group, a reduction in alveolar septal wall thickness and decreased vascular congestion in the interstitial areas were observed. In addition, alveolar (a) structures composed of morphologically typical type I pneumocytes (arrow) and type II pneumocytes (arrowhead) were identified (LDS: 0.5 [0–2]). K (×20)-L (×40): In sections from the CLP+CR20 mg treatment group, reduced alveolar septal wall thickness was observed, together with alveolar (a) structures composed of morphologically typical type I pneumocytes (arrow) and type II pneumocytes (arrowhead) (LDS: 1 [0–1]).

Table 5. Lung damage scores (LDS, Matute-Bello et al.) of the experimental groups.

Group	**Alveolar İnflammation**	Interstitial Inflammation	Vascular Congestion	**LDS**
Sham	0(0-0)	0(0-0)	0(0-0)	0(0-0.5)
Sham + 10 mg/kg Rosuvastatin	0(0-0)	0(0-0)[b]	0(0-0)[b]	0(0-1)[b]
Sham + 20 mg/kg Rosuvastatin	0(0-0)	0(0-1)[c]	0(0-1)[b]	1(0-1)[b]
CLP	1(0-1)[a]	1(1-2)[a]	2(1-2)[a]	5(4-7)[a]
CLP + 10 mg/kg Rosuvastatin	0(0-1)	0(0-1)[d]	0(0-1)[b]	0.5(0-2)[b]
CLP + 20 mg/kg Rosuvastatin	0(0-0)	0(0-1)[e]	0(0-0)[b]	1(0-1)[b]

[a]p=0.000; Compared with the sham group

[b]p=0.000; Compared with the CLP group

[c]p=0.004; Compared with the CLP group

[d]p=0.002; Compared with the CLP group

[e]p=0.001; Compared with the CLP group

Kruskal Wallis/ Tamhane T2 test

Table 6 presents the alveolar septal wall thickness values of rat lung tissue as the arithmetic mean ± standard deviation (mean ± SD). The fold changes relative to the sham group were also determined. In the CLP group, septal wall thickness exhibited an almost threefold increase, whereas administration of rosuvastatin resulted in an average reduction of approximately 1.5-fold. Nevertheless, no statistically significant differences were observed among the various rosuvastatin dosage groups.

 doi:10.20944/preprints202605.0139.v1

Table 6. Alveolar septum thickness.

Group	Alveolar Septal Wall Thickness **(μm)**	Alveolar Septum Thickness (Treatment Group/Control Group)	Alveolar Septum Thickness Score (Matute-Bello et al.)
Sham	8.06±1.68	1	0 (<X2)
Sham + 10 mg/kg Rosuvastatin	9.91±2.15^{b}	1.22	0 (<X2)
Sham + 20 mg/kg Rosuvastatin	9.71±1.81^{b}	1.2	0 (>X2)
CLP	23.75±7.87^{a}	2.94	2 (≥ X2)
CLP + 10 mg/kg Rosuvastatin	12.05±2.38^{b}	1.50	0 (<X2)
CLP + 20 mg/kg Rosuvastatin	12.93±2.85^{b}	1.60	0 (<X2)

Statistical significance is shown as median + standard deviation.

The alveolar septal thickness ratio in the sham group was designated as 1.

[a]p=0.000; Compared with the sham group

[b]p=0.000; Compared with the CLP group

One-Way ANOVA/Tukey HSD test

3.4. Immunohistochemical Results

The immunohistochemical positivity scores for the antibodies used are presented in Table 7. In the CLP group, the scores of all antibodies were significantly higher compared to the other groups. Administration of rosuvastatin in septic animal models resulted in a significant reduction of these scores. The positivity scores of NF-κB/p65, caspase-3, and 8-OHdG antibodies did not show an important difference between the 10 mg and 20 mg rosuvastatin groups.

Table 7. Immunohistochemical positivity score results (median with 25% and 75% interquartile range).

Group	Caspase-3 Positivity Score	NF-kB/p65 Positivity Score	8-OHdG Positivity Score
Sham	0(0-0)	0(0-0)	0(0-0)
Sham + 10 mg/kg Rosuvastatin	0(0-0)	0(0-0)	0(0-1)
Sham + 20 mg/kg Rosuvastatin	0(0-0)	0(0-1)	0(0-1)
CLP	$3(3-3)^{a}$	$3(3-3)^{a}$	$3(2-3)^{a}$
CLP + 10 mg/kg Rosuvastatin	$0.5(0-1)^{b}$	$0(0-1)^{b}$	$0(0-1)^{b}$
CLP + 20 mg/kg Rosuvastatin	$0(0-1)^{b}$	$1(0-1)^{b}$	$0(0-1)^{b}$

 doi:10.20944/preprints202605.0139.v1

[a]p=0.000; Compared with the sham group

[b]p=0.000; Compared with the CLP group

Kruskal Wallis/Tamhane T2

Representative photomicrographs of lung sections immunolabeled for caspase-3 are shown in Figure 3. In sections from the CLP group, numerous pneumocytes within the alveolar septa exhibited intense caspase-3 immunoreactivity, with prominent cytoplasmic and occasional perinuclear localization consistent with apoptotic morphology (arrowheads). In contrast, lungs from rosuvastatin-treated septic rats contained markedly fewer caspase-3–positive cells, and staining intensity was substantially attenuated.

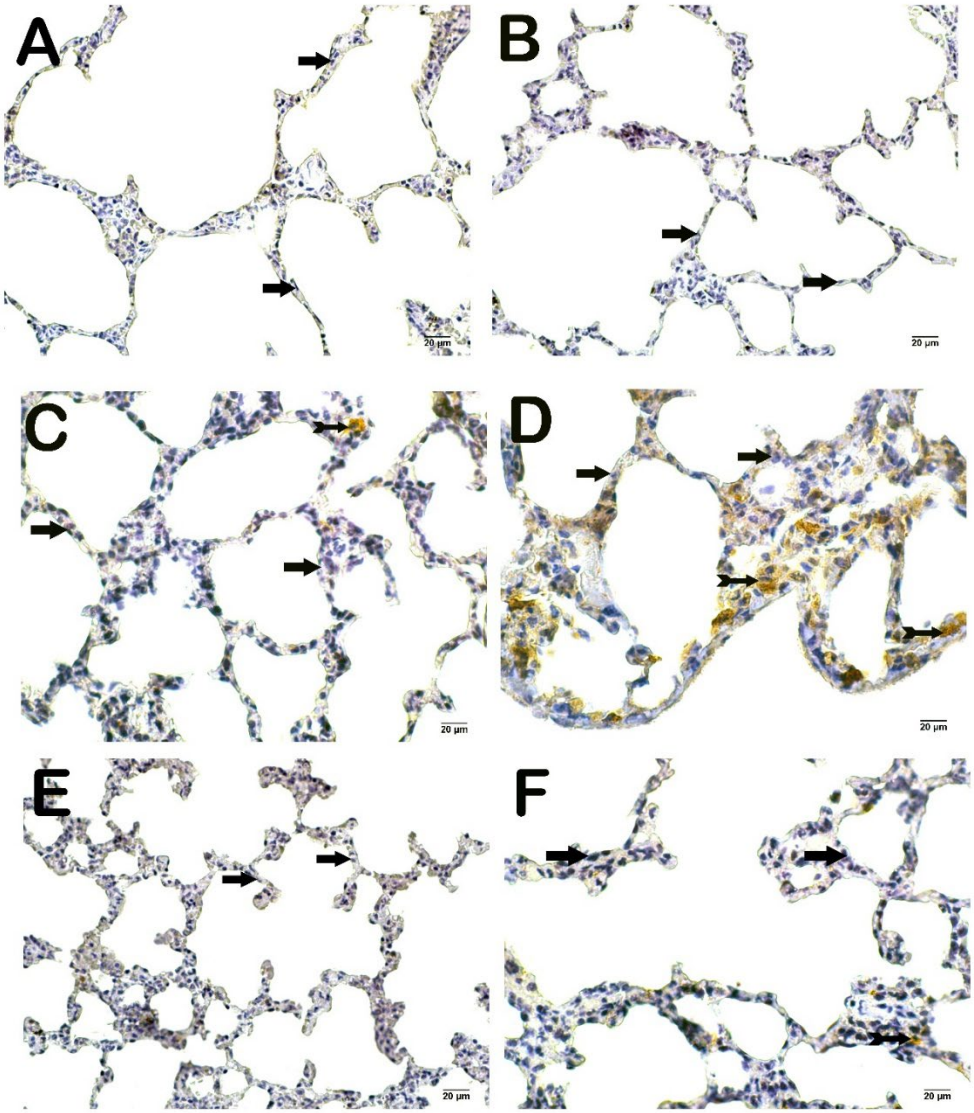

Figure 3. Light microscopic image of lung tissue sections incubated with caspase-3. Positive cells are marked with arrowheads, whereas normal cells are indicated by straight arrows. A: Sham, B: Sham + 10 mg/kg Rosuvastatin, C: Sham + 20 mg/kg Rosuvastatin, D: CLP, E: CLP + 10 mg/kg Rosuvastatin, F: CLP + 20 mg/kg Rosuvastatin.

 doi:10.20944/preprints202605.0139.v1

Representative images of lung sections immunostained for NF-κB/p65 are presented in Figure 4. Sections from the CLP group showed abundant NF-κB/p65–immunopositive pneumocytes (arrowheads), whereas rosuvastatin-treated septic rats displayed a reduced number of NF-κB/p65–positive pneumocytes compared with the CLP group.

Figure 5 shows representative images of lung tissue sections probed with anti–8-OHdG antibodies. The CLP group displayed the highest 8-OHdG signal, with expression significantly elevated relative to all other groups. In the rosuvastatin-treated groups, the number of 8-OHdG–positive pneumocytes was markedly reduced, and no significant differences were observed between the administered doses.

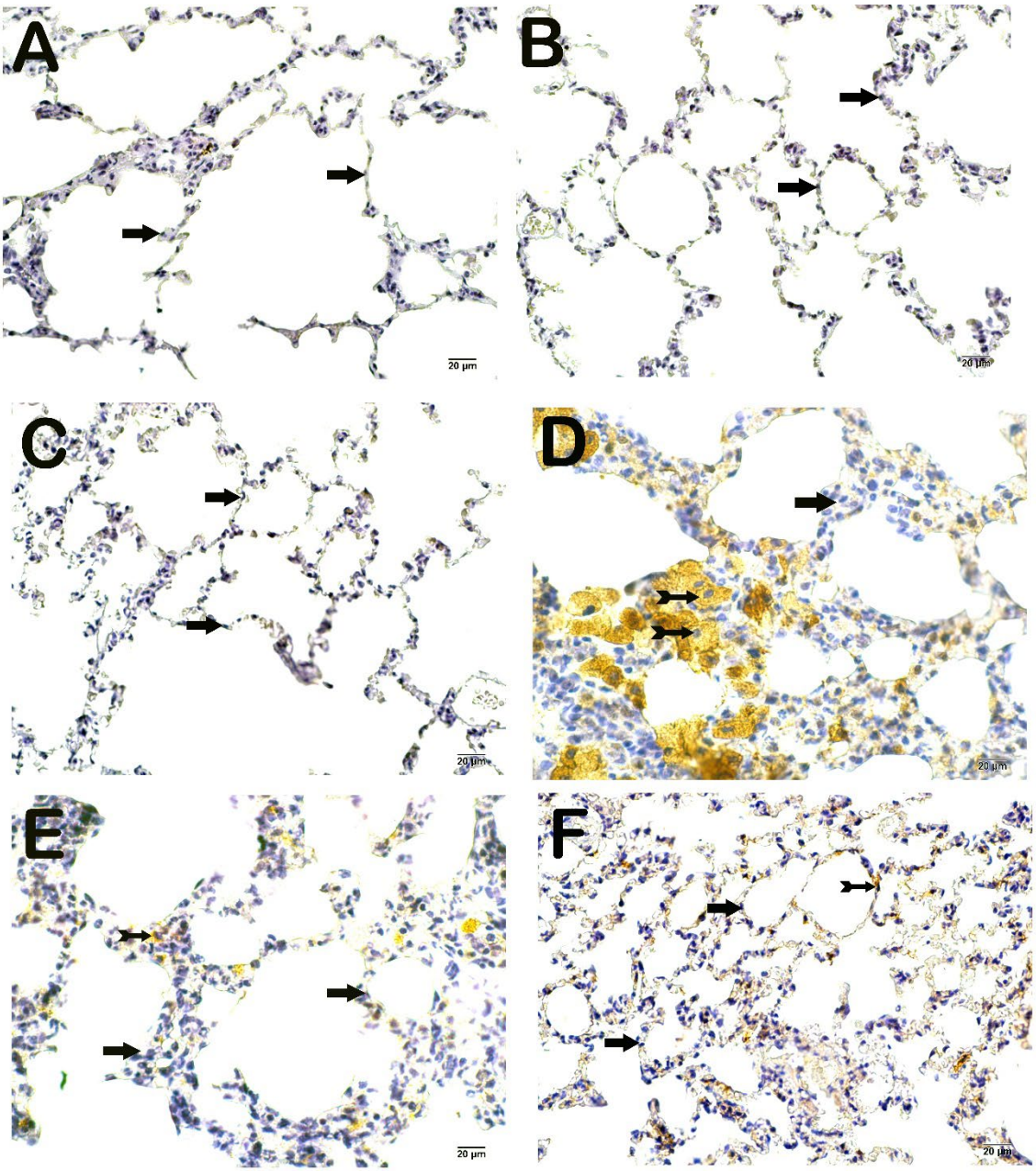

Figure 4. Light microscopic image of lung tissue sections incubated with NF-kβ/p65. Positive cells are marked with arrowheads, whereas normal cells are indicated by straight arrows. **A:** Sham**, B:** Sham + 10 mg/kg Rosuvastatin, **C:** Sham + 20 mg/kg Rosuvastatin, **D:** CLP, **E:** CLP + 10 mg/kg Rosuvastatin, **F**: CLP + 20 mg/kg Rosuvastatin.

 doi:10.20944/preprints202605.0139.v1

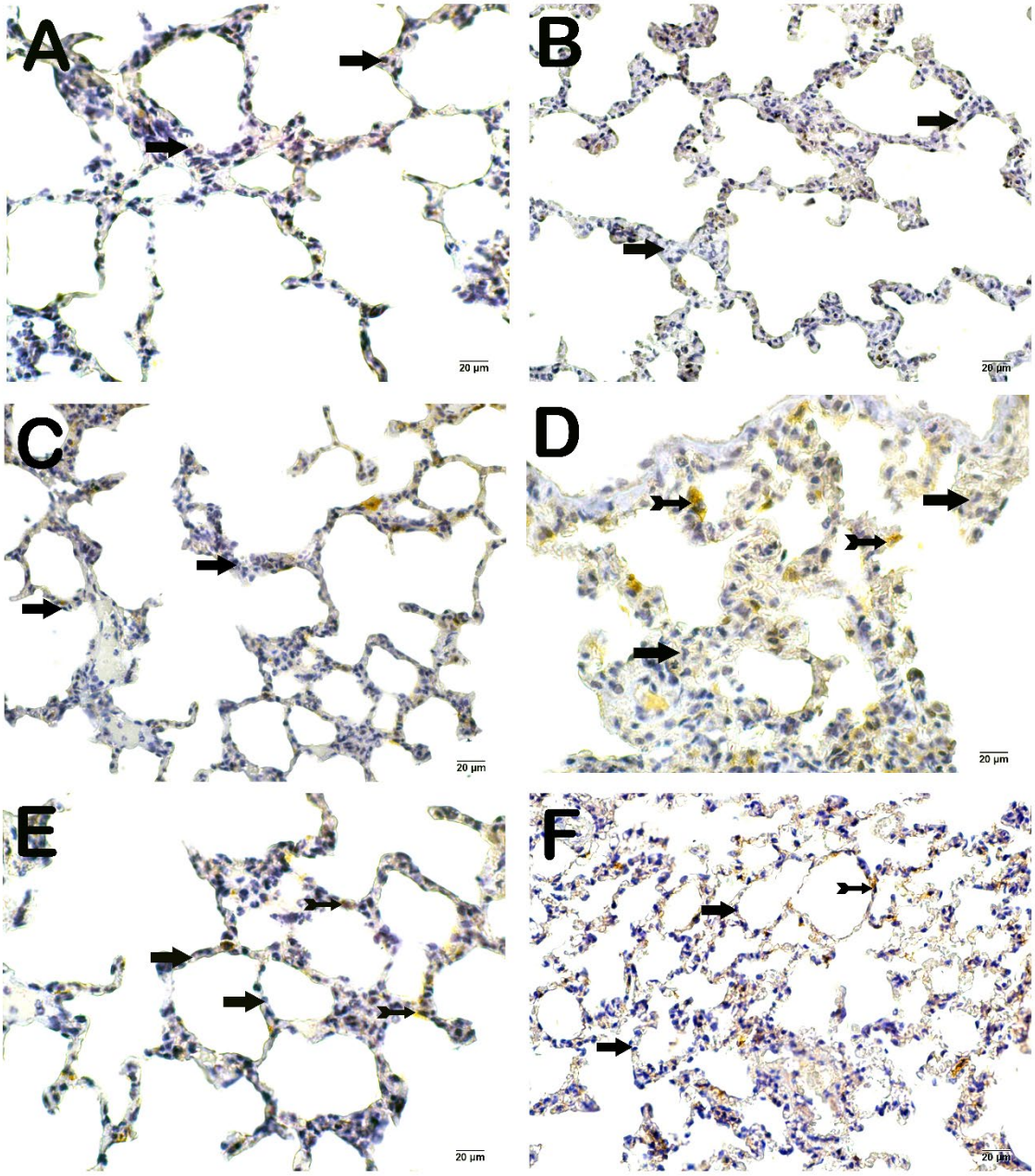

Figure 5. Light microscopic image of lung tissue sections incubated with 8-OHdG. Positive cells are marked with arrowheads, whereas normal cells are indicated by straight arrows. **A:** Sham**, B:** Sham + 10 mg/kg Rosuvastatin, **C:** Sham + 20 mg/kg Rosuvastatin, **D:** CLP, **E:** CLP + 10 mg/kg Rosuvastatin, **F**: CLP + 20 mg/kg Rosuvastatin.

4. Discussion

Despite numerous proposed mechanisms, the pathophysiology of sepsis remains incompletely elucidated. Nevertheless, it is well established that a dysregulated host immune response to infection drives tissue injury. Immune cells recruited to sites of inflammation augment the synthesis and levels of pro-inflammatory cytokines, thereby precipitating cellular damage within organs [28]. Pro-inflammatory cytokines promote the generation of reactive oxygen species (ROS), thereby inducing oxidative stress and consequent tissue injury. In sepsis, the lung is a primary target of this injury and one of the most frequently affected organs. Malondialdehyde (MDA), a lipid peroxidation product

 doi:10.20944/preprints202605.0139.v1

and a key biomarker of tissue-level oxidative stress, has been reported to increase in the lung following induction of sepsis [29]. Reduced glutathione (GSH) is the cell's foremost non-enzymatic antioxidant. Serving primarily as an electron donor for glutathione peroxidase (GPx), it detoxifies peroxides and helps neutralize superoxide and hydroxyl radicals [30].

The documented antioxidant, anti-inflammatory, and immunomodulatory properties of statins have motivated their evaluation as adjunctive or alternative therapeutic strategies for chronic diseases. Rosuvastatin exhibits high affinity for the active site of HMG-CoA reductase and demonstrates superior in vitro potency in inhibiting enzymatic activity and cholesterol biosynthesis relative to other statins [21].

In rat models of sepsis induced by CLP, it has been reported that MDA levels in lung tissue are significantly increased, whereas GSH levels are decreased. Various compounds have been shown to attenuate sepsis-induced pulmonary injury by decreasing MDA levels and increasing GSH levels [4,31,32]. However, the potential effect of rosuvastatin on these oxidative stress parameters in lung tissue has not been clearly demonstrated in animal models of sepsis. In the present study, the elevated MDA levels and decreased GSH levels observed in the sepsis group were significantly reversed following rosuvastatin administration. These findings suggest that rosuvastatin exerts a protective effect against sepsis-induced oxidative damage in lung tissue.

In a study evaluating rosuvastatin's antioxidant effects, rats were exposed to the toxicant fipronil to induce hepatic and renal oxidative injury. Abdel-Daim et al. administered rosuvastatin (10 mg/kg, oral, 15 days) and measured oxidative and antioxidant markers. Rosuvastatin significantly lowered fipronil-elevated MDA and restored depleted GSH in both organs. Fipronil also enhanced caspase-3 expression in hepatic and renal tissues; co-administration of oral rosuvastatin with vitamin E attenuated this apoptosis-associated upregulation [33]. In a separate study conducted in myocardial tissue, azithromycin administration elevated malondialdehyde (MDA) levels, which were reduced by maintenance-dose rosuvastatin (2 mg/kg), while glutathione (GSH) levels increased. Concurrently, the azithromycin-induced upregulation of caspase-3 expression was attenuated by rosuvastatin [34]. Consistent with these reports, rosuvastatin in our study conferred protection to lung tissue under heightened oxidative stress by reducing MDA levels and significantly increasing GSH. Thus, we confirm rosuvastatin's antioxidant effect in sepsis-induced lung injury, extending prior evidence to pulmonary tissue.

In sepsis, NF-κB/p65 is central to TLR-mediated signaling: nuclear translocation of p65 triggers transcription of TNF-α, IL-1β, IL-6, and iNOS/COX-2. This program amplifies neutrophil recruitment, oxidative stress, and epithelial apoptosis, culminating in diffuse alveolar injury. Apoptosis of alveolar epithelial and capillary endothelial cells leads to barrier dysfunction, proteinaceous edema, and impaired gas exchange. Caspase-3, a principal executioner caspase, occupies a central position in the pathophysiology of sepsis. By integrating inputs from the intrinsic (caspase-9–dependent) and extrinsic (caspase-8–dependent) pathways, it orchestrates and carries out the terminal proteolytic events that execute the apoptotic program [35,36].

As one of the earliest organs affected during sepsis, the lung undergoes disruption of tissue integrity because of marked neutrophil infiltration within the pulmonary epithelium, leading to alveolar inflammation, interstitial inflammation, and vascular congestion. In addition, alveolar septal thickness is one of the histopathological features that is markedly altered and commonly evaluated in sepsis.[27]. It has been reported that, in the CLP-induced sepsis group in which these histopathological features were analyzed, both the lung injury score (LDS) and alveolar septal thickness were significantly increased. [24,37]. Our histopathological analysis based on the scoring system of Matute-Bello et al., the lung injury score (LDS) was 0 (0–0.5) in the Sham group and 5 (4–7) in the CLP group. Following administration of rosuvastatin at 10 mg, this value decreased significantly to 0.5 (0–2), whereas treatment with 20 mg rosuvastatin reduced it to 1 (0–1). When the alveolar septal thickness ratio in the Sham group was accepted as 1, this ratio was determined to be 2.94 in the CLP group, 1.50 in the group treated with 10 mg rosuvastatin, and 1.60 in the group treated with 20 mg rosuvastatin. Our findings indicate that rosuvastatin exerts a protective effect against

 doi:10.20944/preprints202605.0139.v1

sepsis-induced acute lung injury (ALI); however, this effect appears to be dose-independent. Further studies are needed to validate and support these findings.

In a recently published study, increased expression of TNF-α and NF-κB in lung tissues of a rat sepsis model was reported [4]. Consistent findings have also been documented in earlier studies evaluating various compounds [31,38]. In a murine model of sepsis, increased TNF-α expression in cortical tissues has been reported, and rosuvastatin was shown to significantly attenuate this elevation [2]. Similarly, in the peritoneal lavage supernatants of the same model, elevated TNF-α levels were significantly reduced following rosuvastatin administration [15]. Mărginean et al. compared the anti-inflammatory effects of rosuvastatin and simvastatin in a rat model of CLP. The statins were administered 18 and 3 hours before surgery, and serum levels of procalcitonin and cytokines (IL-1β, IL-6, and TNF-α) were measured. Both rosuvastatin and simvastatin demonstrated significant anti-inflammatory activity in this sepsis model [39]. In another study, lung tissue samples from the CLP-induced sepsis group exhibited markedly elevated NF-κB/p65 expression, which was significantly reduced following fosfomycin administration [24]. In our study, TNF-α and NF-κB/p65 levels were elevated in the sepsis group, whereas this increase was significantly attenuated in the rosuvastatin-treated group. These results further support the notion that rosuvastatin exerts modulatory effects on inflammatory pathways contributing to sepsis-induced lung injury.

8-OHdG is elevated in sepsis at both systemic (serum/urine) and pulmonary tissue levels, parallels indices of oxidative stress and lipid peroxidation (e.g., malondialdehyde, MDA), and correlates with disease severity and mortality. These findings support 8-OHdG as a reliable biomarker of oxidative DNA damage in sepsis and a useful pharmacodynamic readout for monitoring the impact of antioxidant or anti-inflammatory interventions [40]. In a study using a CLP-induced sepsis/ALI model in rats, 8-OHdG levels were evaluated in lung tissue. The authors reported that 8-OHdG levels were elevated in the CLP group, whereas resveratrol treatment attenuated this elevation by 41%. Another study employing the same model, in which 8-OHdG immunopositivity was assessed, likewise reported increased 8-OHdG levels in the sepsis group and demonstrated that costunolide treatment reduced this marker [41]. However, the effect of rosuvastatin on oxidative DNA damage in lung tissue has not previously been demonstrated. In our experimental groups, 8-OHdG levels were evaluated by immunohistochemical analysis. The increased positivity scores observed in the lung tissues of the sepsis group showed a statistically significant reduction following administration of rosuvastatin at doses of 10 mg and 20 mg. Nevertheless, no significant difference was detected between the two treatment doses. Our findings regarding 8-OHdG levels indicate that rosuvastatin also exerts a protective effect on the cellular pathways involved in oxidative DNA damage.

Rosuvastatin has been shown to inhibit apoptotic pathways in multiple tissues, including the liver, kidney, and myocardium [33,34]. Extending this evidence to the lung, we demonstrate an anti-apoptotic effect in the clinically relevant setting of sepsis, as evidenced by reduced caspase-3 expression. Caspase-3 levels, which were elevated in the CLP group, declined markedly after rosuvastatin treatment, without a discernible dose-dependent difference.

Our study had several limitations. First, sepsis is a systemic condition that affects not only the lungs but also the circulatory system and other organs, including the liver, kidneys, and spleen. Therefore, analysis of these organs would be necessary to comprehensively evaluate the overall effects of rosuvastatin. In addition, oxidative stress, inflammation, apoptosis, and oxidative DNA damage pathways were assessed using a limited number of biomarkers in the present study. Evaluation of additional key markers involved in these pathways would be required to further validate our findings. Moreover, tissue integrity was examined at the microscopic level; however, assessment of intercellular junction molecules at the molecular level could have provided more direct evidence regarding the effects of rosuvastatin. Rosuvastatin was administered exclusively as a prophylactic treatment, 4 hours before sepsis induction. Additional experimental designs incorporating post-sepsis treatment regimens would enhance the clinical relevance and translational value of our findings.

 doi:10.20944/preprints202605.0139.v1

5. Conclusions

Although studies investigating the effects of rosuvastatin in experimental sepsis models remain limited, the available evidence suggests that this agent has anti-inflammatory potential. In this regard, our findings indicating the biochemical and histological protective effects of rosuvastatin in a CLP-induced sepsis model in rats are noteworthy. Nevertheless, in addition to further studies targeting a broader spectrum of cellular signaling pathways, therapeutic rather than prophylactic models are also required to fully elucidate the protective potential and clinical applicability of rosuvastatin in sepsis. Additionally, when the two different doses of rosuvastatin (10 mg/kg and 20 mg/kg) were compared across all analyzed parameters, no significant difference was observed between the dose groups. This finding indicates that rosuvastatin did not exhibit a dose-dependent effect under the conditions of the present study. Given the therapeutically challenging nature of sepsis, characterized by complex pathophysiology and high mortality, the demonstration of a therapeutic effect of a widely used drug such as rosuvastatin represents an important finding.

Author Contributions: Conceptualization, S.İ.Y. and F.S.; Methodology, S.İ.Y and E.Y.K; Validation, A.T. and F.S.; Formal Analysis, E.Y.K.; Investigation, S.İ.Y.; Resources, S.İ.Y.; Data Curation, A.T. and L.T.; Writing – Original Draft Preparation, L.T and F.S.; Writing – Review & Editing, H.A.U; Visualization, H.A.U. and L.T.; Supervision, F.S.; Project Administration, H.A.U and F.S.; Funding Acquisition, F.S.

Institutional Review Board Statement: The study was conducted in accordance with the Declaration of Helsinki and approved by the Laboratory Animals Institutional Ethical Committee of Recep Tayyip Erdogan University (Protocol Code: 2020/32, Date of approval: 16.07.2020).

Funding: This study was supported by the Scientific Research Projects Unit of Recep Tayyip Erdoğan University (Project No. TYL-2021-1289) and the Recep Tayyip Erdoğan University Development Foundation (Grant No. 02026003030216).

Conflicts of Interest: The authors declared no potential conflicts of interest with respect to the research, authorship, and/or publication of this article.

Data Availability Statement: The data that support the findings of this study are available from the corresponding author upon reasonable request.

Abbreviations

The following abbreviations are used in this manuscript:

ALI	Acute lung injury
CLP	Cecal ligation and puncture
MDA	Malondialdehyde
GSH	Reduced glutathione
ARDS	Acute respiratory distress syndrome
NF-κB/p65	Nuclear factor kappa B/65
TNF-α	Tumor necrosis factor-alpha
IL-6	Interleukin-6
IL-1β	Interleukin-1 beta
IL-10	Interleukin-10
ROS	Reactive oxygen species
SOD	Superoxide dismutase

 doi:10.20944/preprints202605.0139.v1

GR	Glutathione reductase
GSH-Px	Glutathione peroxidase
CAT	Catalase
RNS	Reactive nitrogen species
8-OHdG	8-hydroxy-2′-deoxyguanosine
HMG-CoA	Hydroxy-3-methylglutaryl-CoA
TBARS	Thiobarbituric acid-reactive substances
DTNB	5,5-dithiobis-(2-nitrobenzoic acid)
H&E	Hematoxylin-Eosin
LDS	Lung damage score
IHC	Immunohistochemical

References

1. Singer, M.; Deutschman, C. S.; Seymour, C. W.; Shankar-Hari, M.; Annane, D.; Bauer, M.; Bellomo, R.; Bernard, G. R.; Chiche, J. D.; Coopersmith, C. M.; Hotchkiss, R. S.; Levy, M. M.; Marshall, J. C.; Martin, G. S.; Opal, S. M.; Rubenfeld, G. D.; van der Poll, T.; Vincent, J. L.; Angus, D. C., The Third International Consensus Definitions for Sepsis and Septic Shock (Sepsis-3). *JAMA* **2016,** *315* (8), 801-10.
2. Shen, Q.; Yu, Q.; Chen, T.; Zhang, L., Rosuvastatin mitigates blood-brain barrier disruption in sepsis-associated encephalopathy by restoring occludin levels. *Eur J Med Res* **2025,** *30* (1), 103.
3. Vella, R.; Panci, D.; Carini, F.; Malta, G.; Vieni, S.; David, S.; Albano, G. D.; Puntarello, M.; Zerbo, S.; Argo, A., Cytokines in sepsis: a critical review of the literature on systemic inflammation and multiple organ dysfunction. *Front Immunol* **2025,** *16*, 1682306.
4. Bati, Y. U.; Sezer, M.; Yilmaz, A.; Baser, L.; Guraslan, A.; Bayram, P.; Karamese, M., The Protective Effects of Dose-Dependent Umbelliferone Application on CLP-Induced Acute Lung Injury (ALI) Model. *J Biochem Mol Toxicol* **2025,** *39* (10), e70549.
5. Huang, M.; Cai, S.; Su, J., The Pathogenesis of Sepsis and Potential Therapeutic Targets. *Int J Mol Sci* **2019,** *20* (21).
6. Sun, B.; Lei, M.; Zhang, J.; Kang, H.; Liu, H.; Zhou, F., Acute lung injury caused by sepsis: how does it happen? *Front Med (Lausanne)* **2023,** *10*, 1289194.
7. Exline, M. C.; Crouser, E. D., Mitochondrial mechanisms of sepsis-induced organ failure. *Front Biosci* **2008,** *13*, 5030-41.
8. Chopra, M.; Reuben, J. S.; Sharma, A. C., Acute lung injury:apoptosis and signaling mechanisms. *Exp Biol Med (Maywood)* **2009,** *234* (4), 361-71.
9. Herrero, R.; Sanchez, G.; Lorente, J. A., New insights into the mechanisms of pulmonary edema in acute lung injury. *Ann Transl Med* **2018,** *6* (2), 32.
10. Dragoescu, A. N.; Padureanu, V.; Stanculescu, A. D.; Andrei, M.; Radu, M.; Padureanu, R.; Iliescu, D. G.; Dragoescu, P. O., Perioperative Oxidative Stress and Sepsis: Pathophysiological and Clinical Implications. *Cureus* **2025,** *17* (10), e94719.
11. da Silva Sergio, L. P.; Mencalha, A. L.; de Souza da Fonseca, A.; de Paoli, F., DNA repair and genomic stability in lungs affected by acute injury. *Biomed Pharmacother* **2019,** *119*, 109412.
12. Liu, X.; Deng, K.; Chen, S.; Zhang, Y.; Yao, J.; Weng, X.; Zhang, Y.; Gao, T.; Feng, G., 8-Hydroxy-2'-deoxyguanosine as a biomarker of oxidative stress in acute exacerbation of chronic obstructive pulmonary disease. *Turk J Med Sci* **2019,** *49* (1), 93-100.
13. Nedel, W.; Deutschendorf, C.; Portela, L. V. C., Sepsis-induced mitochondrial dysfunction: A narrative review. *World J Crit Care Med* **2023,** *12* (3), 139-152.

 doi:10.20944/preprints202605.0139.v1

14. Srdic, T.; Durasevic, S.; Lakic, I.; Ruzicic, A.; Vujovic, P.; Jevdovic, T.; Dakic, T.; Dordevic, J.; Tosti, T.; Glumac, S.; Todorovic, Z.; Jasnic, N., From Molecular Mechanisms to Clinical Therapy: Understanding Sepsis-Induced Multiple Organ Dysfunction. *Int J Mol Sci* **2024,** *25* (14).
15. Rittirsch, D.; Huber-Lang, M. S.; Flierl, M. A.; Ward, P. A., Immunodesign of experimental sepsis by cecal ligation and puncture. *Nat Protoc* **2009,** *4* (1), 31-6.
16. Rachoin, J. S.; Cerceo, E.; Dellinger, R. P., A new role for statins in sepsis. *Crit Care* **2013,** *17* (1), 105.
17. Gao, F.; Linhartova, L.; Johnston, A. M.; Thickett, D. R., Statins and sepsis. *Br J Anaesth* **2008,** *100* (3), 288-98.
18. Liappis, A. P.; Kan, V. L.; Rochester, C. G.; Simon, G. L., The effect of statins on mortality in patients with bacteremia. *Clin Infect Dis* **2001,** *33* (8), 1352-7.
19. Li, M.; Noordam, R.; Trompet, S.; Winter, E. M.; Jukema, J. W.; Arbous, M. S.; Rensen, P. C. N.; Kooijman, S., The impact of statin use on sepsis mortality. *J Clin Lipidol* **2024,** *18* (6), e915-e925.
20. Cortese, F.; Gesualdo, M.; Cortese, A.; Carbonara, S.; Devito, F.; Zito, A.; Ricci, G.; Scicchitano, P.; Ciccone, M. M., Rosuvastatin: Beyond the cholesterol-lowering effect. *Pharmacol Res* **2016,** *107*, 1-18.
21. Saadat, S.; Mohamadian Roshan, N.; Aslani, M. R.; Boskabady, M. H., Rosuvastatin suppresses cytokine production and lung inflammation in asthmatic, hyperlipidemic and asthmatic-hyperlipidemic rat models. *Cytokine* **2020,** *128*, 154993.
22. Ren, G.; Zhou, Q.; Lu, M.; Wang, H., Rosuvastatin corrects oxidative stress and inflammation induced by LPS to attenuate cardiac injury by inhibiting the NLRP3/TLR4 pathway. *Can J Physiol Pharmacol* **2021,** *99* (9), 964-973.
23. Tang, Z.; Ning, Z.; Li, Z., The beneficial effects of Rosuvastatin in inhibiting inflammation in sepsis. *Aging (Albany NY)* **2024,** *16* (12), 10424-10434.
24. Yildiz, I. E.; Topcu, A.; Bahceci, I.; Arpa, M.; Tumkaya, L.; Mercantepe, T.; Batcik, S.; Yildiz, Y., The protective role of fosfomycin in lung injury due to oxidative stress and inflammation caused by sepsis. *Life Sci* **2021,** *279*, 119662.
25. Ohkawa, H.; Ohishi, N.; Yagi, K., Assay for lipid peroxides in animal tissues by thiobarbituric acid reaction. *Anal Biochem* **1979,** *95* (2), 351-8.
26. Ellman, G. L., Tissue sulfhydryl groups. *Arch Biochem Biophys* **1959,** *82* (1), 70-7.
27. Matute-Bello, G.; Downey, G.; Moore, B. B.; Groshong, S. D.; Matthay, M. A.; Slutsky, A. S.; Kuebler, W. M.; Acute Lung Injury in Animals Study, G., An official American Thoracic Society workshop report: features and measurements of experimental acute lung injury in animals. *Am J Respir Cell Mol Biol* **2011,** *44* (5), 725-38.
28. Gyawali, B.; Ramakrishna, K.; Dhamoon, A. S., Sepsis: The evolution in definition, pathophysiology, and management. *SAGE Open Med* **2019,** *7*, 2050312119835043.
29. Kumar, V., Pulmonary Innate Immune Response Determines the Outcome of Inflammation During Pneumonia and Sepsis-Associated Acute Lung Injury. *Front Immunol* **2020,** *11*, 1722.
30. Hu, Q.; Wang, Q.; Han, C.; Yang, Y., Sufentanil attenuates inflammation and oxidative stress in sepsis-induced acute lung injury by downregulating KNG1 expression. *Mol Med Rep* **2020,** *22* (5), 4298-4306.
31. Senousy, S. R.; Ahmed, A. F.; Abdelhafeez, D. A.; Khalifa, M. M. A.; Abourehab, M. A. S.; El-Daly, M., Alpha-Chymotrypsin Protects Against Acute Lung, Kidney, and Liver Injuries and Increases Survival in CLP-Induced Sepsis in Rats Through Inhibition of TLR4/NF-kappaB Pathway. *Drug Des Devel Ther* **2022,** *16*, 3023-3039.
32. Gerin, F.; Sener, U.; Erman, H.; Yilmaz, A.; Aydin, B.; Armutcu, F.; Gurel, A., The Effects of Quercetin on Acute Lung Injury and Biomarkers of Inflammation and Oxidative Stress in the Rat Model of Sepsis. *Inflammation* **2016,** *39* (2), 700-5.
33. Abdel-Daim, M. M.; Abdeen, A., Protective effects of rosuvastatin and vitamin E against fipronil-mediated oxidative damage and apoptosis in rat liver and kidney. *Food Chem Toxicol* **2018,** *114*, 69-77.
34. Mansour, B. S.; Salem, N. A.; Kader, G. A.; Abdel-Alrahman, G.; Mahmoud, O. M., Protective effect of Rosuvastatin on Azithromycin induced cardiotoxicity in a rat model. *Life Sci* **2021,** *269*, 119099.
35. Porter, A. G.; Janicke, R. U., Emerging roles of caspase-3 in apoptosis. *Cell Death Differ* **1999,** *6* (2), 99-104.

 doi:10.20944/preprints202605.0139.v1

36. Martin, T. R.; Hagimoto, N.; Nakamura, M.; Matute-Bello, G., Apoptosis and epithelial injury in the lungs. *Proc Am Thorac Soc* **2005,** *2* (3), 214-20.
37. Sahin, K.; Sahin Aktura, S.; Bahceci, I.; Mercantepe, T.; Tumkaya, L.; Topcu, A.; Mercantepe, F.; Duran, O. F.; Uydu, H. A.; Yazici, Z. A., Is Punica granatum Efficient Against Sepsis? A Comparative Study of Amifostine Versus Pomegranate. *Life (Basel)* **2025,** *15* (1).
38. Cadirci, E.; Halici, Z.; Odabasoglu, F.; Albayrak, A.; Karakus, E.; Unal, D.; Atalay, F.; Ferah, I.; Unal, B., Sildenafil treatment attenuates lung and kidney injury due to overproduction of oxidant activity in a rat model of sepsis: a biochemical and histopathological study. *Clin Exp Immunol* **2011,** *166* (3), 374-84.
39. Mărginean M, M.; Trancă, S.; Ardelean-Maghiar, A.; Dîrzu, D.; Huțanu, A.; Platon, O.; Dobreanu, D., Comparing the anti-inflammatory effects of Simvastatin and Rosuvastatin by measuring IL-1β, IL-6 and TNF-α levels using a murinic caecal ligation and puncture induced sepsis model / Compararea efectelor anti-inflamatoare ale Simvastatinei și Rosuvastatinei măsurând nivelele serice ale IL-1β, IL-6 si TNF-α folosind un model de sepsis la șobolan indus prin ligatură și puncție cecală. *Romanian Review of Laboratory Medicine* **2014,** *22* (4).
40. Lorente, L.; Martin, M. M.; Gonzalez-Rivero, A. F.; Perez-Cejas, A.; Abreu-Gonzalez, P.; Ortiz-Lopez, R.; Ferreres, J.; Sole-Violan, J.; Labarta, L.; Diaz, C.; Palmero, S.; Jimenez, A., Association between DNA and RNA oxidative damage and mortality in septic patients. *J Crit Care* **2019,** *54*, 94-98.
41. Guler, M. C.; Tanyeli, A.; Eraslan, E.; Celebi, O.; Celebi, D.; Comakli, S.; Yurdgulu, E. E.; Bayir, Y., Alleviating sepsis: Revealing the protective role of costunolide in a cecal ligation and puncture rat model. *Iran J Basic Med Sci* **2024,** *27* (5), 567-576.